

Deep Generative Imputation Model for Missing Not At Random Data

Jialei Chen
MIC Lab,
Department of Computer
Science and Technology,
Jilin University
Changchun, China
chenjl21@mails.jlu.edu.cn

Yuanbo Xu*
MIC Lab,
Department of Computer
Science and Technology,
Jilin University
Changchun, China
yuanbox@jlu.edu.cn

Pengyang Wang
SKL-IOTSC,
Department of Computer
and Information Science,
University of Macau
Macao, China
pywang@um.edu.mo

Yongjian Yang
MIC Lab,
Department of Computer
Science and Technology,
Jilin University
Changchun, China
yyj@jlu.edu.cn

ABSTRACT

Data analysis usually suffers from the Missing Not At Random (MNAR) problem, where the cause of the value missing is not fully observed. Compared to the naive Missing Completely At Random (MCAR) problem, it is more in line with the realistic scenario whereas more complex and challenging. Existing statistical methods model the MNAR mechanism by different decomposition of the joint distribution of the complete data and the missing mask. But we empirically find that directly incorporating these statistical methods into deep generative models is sub-optimal. Specifically, it would neglect the confidence of the reconstructed mask during the MNAR imputation process, which leads to insufficient information extraction and less-guaranteed imputation quality. In this paper, we revisit the MNAR problem from a novel perspective that the complete data and missing mask are two modalities of incomplete data on an equal footing. Along with this line, we put forward a generative-model-specific joint probability decomposition method, *conjunction model*, to represent the distributions of two modalities in parallel and extract sufficient information from both complete data and missing mask. Taking a step further, we exploit a deep generative imputation model, namely GNR, to process the real-world missing mechanism in the latent space and concurrently impute the incomplete data and reconstruct the missing mask. The experimental results show that our GNR surpasses state-of-the-art MNAR baselines with significant margins (averagely improved from 9.9% to 18.8% in RMSE) and always gives a better mask reconstruction accuracy which makes the imputation more principle.

CCS CONCEPTS

• **Computing methodologies** → **Maximum likelihood modeling**; *Latent variable models*; • **Information systems** → **Data mining**; • **Mathematics of computing** → *Variational methods*.

*corresponding author

Permission to make digital or hard copies of all or part of this work for personal or classroom use is granted without fee provided that copies are not made or distributed for profit or commercial advantage and that copies bear this notice and the full citation on the first page. Copyrights for components of this work owned by others than the author(s) must be honored. Abstracting with credit is permitted. To copy otherwise, or republish, to post on servers or to redistribute to lists, requires prior specific permission and/or a fee. Request permissions from permissions@acm.org.
CIKM '23, October 21–25, 2023, Birmingham, United Kingdom
© 2023 Copyright held by the owner/author(s). Publication rights licensed to ACM.
ACM ISBN 978-x-xxxx-xxxx-x/YY/MM... \$15.00
<https://doi.org/10.1145/nnnnnnn.nnnnnnn>

KEYWORDS

Missing Data, Missing Not At Random, Imputation; Deep Generative Models, Variational Autoencoder

ACM Reference Format:

Jialei Chen, Yuanbo Xu, Pengyang Wang, and Yongjian Yang. 2023. Deep Generative Imputation Model for Missing Not At Random Data. In *Proceedings of the 32nd ACM International Conference on Information and Knowledge Management (CIKM '23)*, October 21–25, 2023, Birmingham, United Kingdom. ACM, New York, NY, USA, 10 pages. <https://doi.org/10.1145/nnnnnnn.nnnnnnn>

1 INTRODUCTION

In most real-world scenarios, missing data is an inevitable byproduct during the data-generating process, which severely limits the performance of machine learning methods. Being able to impute the missing data unbiasedly requires correct assumptions about the underlying data-generating process, as well as the missing mechanism in deciding which data is missing.

In general, there are three assumptions of missing mechanisms [19, 27]. The first assumption is Missing Completely At Random (MCAR), where the probability of data values missing is independent of both the observed and unobserved (or missing) data. In this case, no statistical bias is introduced to the distribution of complete data. The second assumption is Missing At Random (MAR), where the missing mechanism is independent of the value of unobserved data. Under the MAR assumption, maximum likelihood learning can avoid explicit modeling of missing mechanisms by marginalizing missing data. The third assumption is Missing Not At Random (MNAR), where the missing mechanism depends not only on the observed data but also on the missing data.

Due to the strict restrictions of MAR and MCAR assumptions, the MNAR assumption is more realistic and complicated in many real-world scenarios. For example, people are reluctant to rate uninterested items which leaves a large number of low rating values missing from collected data (Rating 1 in Figure 1) [4]; participants in financial distress are more likely to refuse to complete the survey about financial income. So the cause of missing (hobby or income) can be unobserved and falls under the MNAR mechanism. The distribution of observed and missing data usually manifests discrepancies in MNAR data. Ignoring this discrepancy would result in a serious imputation bias and limits the performance of machine learning methods. Thus the MNAR mechanism must be considered.

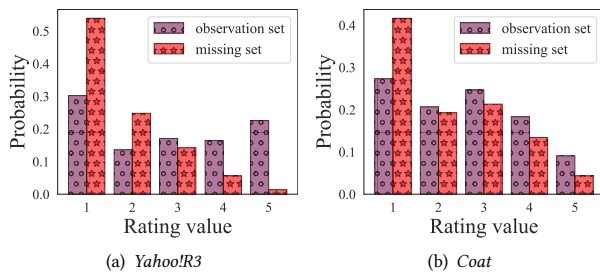


Figure 1: Histogram of the distribution of observed and unobserved (or missing) data shows obvious differences on two five-star rating datasets (*Yahoo!R3* and *Coat*)[¶].

Existing methods for modeling the MNAR mechanism are largely evolved from statistical data analysis by modeling the joint distribution of the complete data and the missing mask. The missing mask is an indicator that reflects whether a value has been observed or unobserved (or missing). According to the different serial decomposition of the joint distribution, they can be divided into the *selection model*, the *pattern-mixture model*, and the *pattern-set mixture model* [19]. In recent progress, selection-model-based methods have risen to prominence and derived several deep generative imputation models for MNAR data [12, 22]. The motivation of the selection-model-based methods is to deduce the missing mechanism in the sample space by mapping the data to the mask, with the assumption that the complete data is the cause of values missing. Thus they utilize a serial structure (top of Figure 2), which involves building an imputation model for presenting the complete data distribution and imputing missing data, followed by reconstructing the mask through a simple mapping of the imputed data.

However, there are main two challenges with selection-model-based deep generative imputation models (with serial structure)^{||}:

- **Low-quality mask reconstruction.** Some values in observed data and missing data (Rating 2,3,4 in Figure 1) usually have a similar probability distribution and are hard to distinguish in the complete data. Mapping the complete (or imputed) data to mask has an information bottleneck and can result in wrong distribution matching (top of Figure 2), which eventually makes the reconstructed mask error as shown in the second row of Figure 5. Since serial structure maps data space to fill a 0 or 1 at some location in the mask, we can abstract this procedure as a classifier. It forces a segmentation of the highly overlapping space of observed and missing data to fit the classification task (mask reconstruction), which is detrimental to the parameter estimation in the data space and eventually leads to biased imputation performance.

- **Neglect of unique information in the missing mask.** Intuitively, the missing mask provides unique information to distinguish observed and missing data (e.g., 0,1 respectively denotes observed and missing). The distribution of the mask can be modeled independently through some carefully-designed structure without

[¶]The two datasets both contain an MNAR set and a small MCAR set. The observation set directly inherits from the MNAR set. Since the MCAR mechanism does not affect the distribution of complete data, we have a unique opportunity to present the distribution of complete data with the MCAR set. We obtain the distribution of the missing set by calculating the difference between the MCAR and MNAR sets.

^{||}The two additional MNAR modeling methods, which also utilize similar serial structures for mapping data space and mask space, encounter comparable problems.

misleading the parameter estimate in the data space. Unfortunately, existing methods ignore the unique information and assume that the complete data contains all the information of the mask further utilizing the serial-structure selection model [6, 12, 22].

To tackle these challenges, we revisit the relationship between the complete data and the missing mask under the assumption that *they are two modalities of missing-data multimodality*. According to the aforementioned drawbacks of directly mapping complete (or imputed) data to the missing mask, we propose a probability decomposition framework, namely *conjunction model*. It can be well-adopted in the generative models to simultaneously model the distribution of the complete data and the missing mask with a parallel structure, which fully mines the information in the two modalities without interfering with each other.

Taking a step further, we incorporate the conjunction model into VAEs and put forward a deep generative imputation model for missing not at random data, namely **GNR**. Specifically, GNR employs a plain encoder to input only the observed data (as obtaining the mask from the observations is intuitive), and two paralleled decoders to reconstruct data space and mask space respectively. The desirable properties of the parallel structure are two-fold: (i) *avoiding the information bottleneck of imputed data during the mask reconstruction*; (ii) *fully extracting the information about the missing mechanism from not only the data space but also the mask space*. In this way, GNR reconstructs the mask with high credibility and quality which contributes to the rational data imputation. Moreover, we theoretically prove the unbiased evidence lower bound of GNR which ensures promising and stable performance on various tasks.

To summarize, our major contributions can be listed as follows:

- We empirically point out that the mask reconstruction in serial-structure methods is sub-optimal, and propose the conjunction model to avoid the information bottleneck and treats the complete data and missing mask as two modalities.
- We put forward a parallel-structure deep generative imputation model based on the conjunction model, namely GNR, to simultaneously impute the missing data unbiasedly and reconstruct the missing mask convincingly.
- We evaluate the imputation performance of our algorithm on 9 datasets (1 synthetic and 8 real-world). GNR achieves state-of-the-art performance on all validated datasets with multiple missing settings (average surpasses MNAR counterparts by 11.65%) and consistently reveals accurate mask reconstruction which makes imputation more guaranteed.

2 PROBLEM SETTING

Similar to the notations introduced by Ghalebikesabi et al. [6] and Yoon et al. [40], Let $\mathbf{x} = (x_1, \dots, x_d)$ be a random variable taking values in the d -dimensional full-observed feature space $\mathcal{X} = \mathcal{X}_1 \times \dots \times \mathcal{X}_d$. To define precisely the observed quantity, we introduce the missing mask vector \mathbf{m} :

$$m_j = \begin{cases} 1 & \text{if } x_j \text{ is observed,} \\ 0 & \text{if } x_j \text{ is missing/unobserved.} \end{cases} \quad (1)$$

Additionally, we introduce the incomplete random variable $\mathbf{x}^{\text{obs}} = (x_1^{\text{obs}}, \dots, x_d^{\text{obs}}) \in \mathcal{X}$ which takes values in $\mathcal{X} = (\mathcal{X}_1 \cup \{*\}) \times \dots \times$

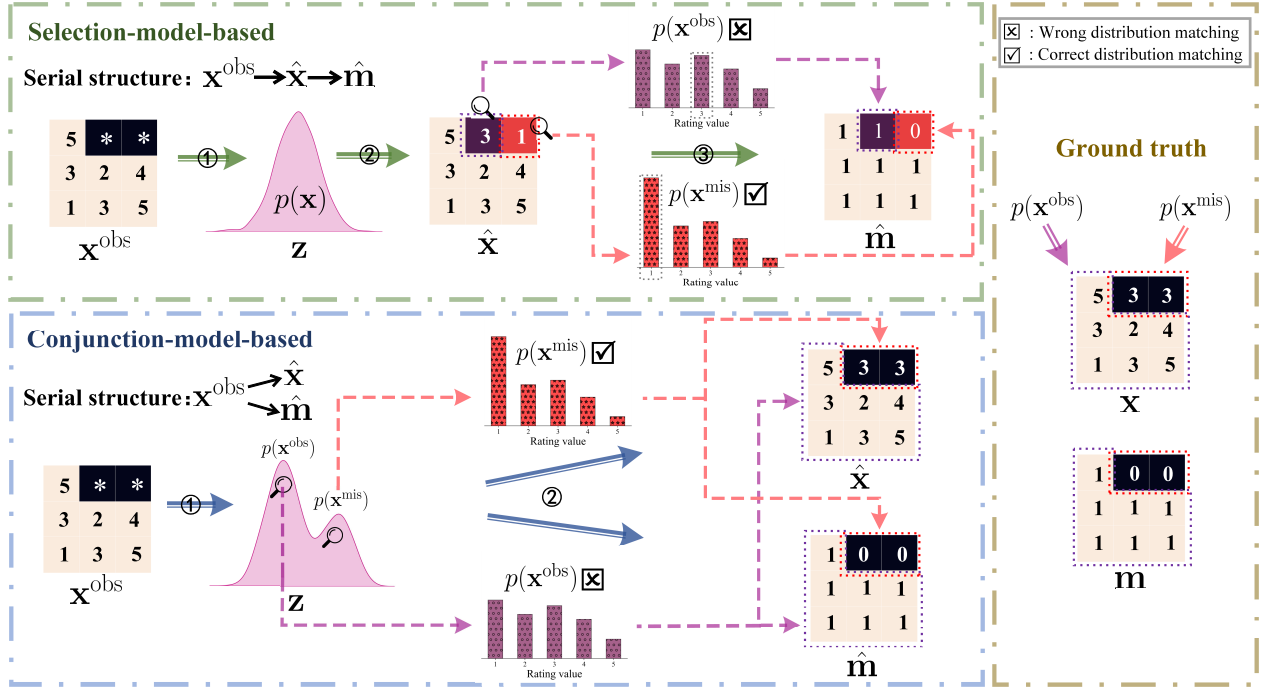


Figure 2: The procedure of inference with deep generative imputation models based on selection model or conjunction model. The selection-model-based methods use a serial structure to fit the definition of Equation 7. The dashed lines are some specific examples of value inference. The reconstructed mask mapping from the imputed data is biased because of the wrong distribution matching. While the conjunction-model-based GNR avoids serial mapping and adopts a parallel structure (Equation 10) to extract the information both in the data space and mask space without interfering with each other.

$(\mathcal{X}_d \cup \{*\})$ where $*$ is a point not in \mathcal{X} and represents unobserved data points. \mathbf{x}^{obs} denotes the set of observed elements of \mathbf{x} . \mathbf{x}^{obs} can be introduced by

$$\mathbf{x}^{\text{obs}} = * \odot (1 - \mathbf{m}) + \mathbf{x} \odot \mathbf{m}, \quad (2)$$

where \odot denotes the Hadamard product. Similarly, we also introduce another random variable \mathbf{x}^{mis} , which refers to the set of missing elements of \mathbf{x} , as follows:

$$\mathbf{x}^{\text{mis}} = * \odot \mathbf{m} + \mathbf{x} \odot (1 - \mathbf{m}). \quad (3)$$

We can now retrieve \mathbf{x} as:

$$\mathbf{x} = \mathbf{x}^{\text{obs}} \odot \mathbf{m} + \mathbf{x}^{\text{mis}} \odot (1 - \mathbf{m}). \quad (4)$$

Suppose that we have the underlying data-generating process, denoted by $p_{\mathcal{D}}(\mathbf{x}^{\text{obs}}, \mathbf{m})$, from which we can obtain (partially observed) samples $(\mathbf{x}^{\text{obs}}, \mathbf{m}) \sim p_{\mathcal{D}}(\mathbf{x}^{\text{obs}}, \mathbf{m})$. We assume that we are given n i.i.d. samples of \mathbf{x}^{obs} . The dataset collected by the deployed system can be defined as $\mathcal{D} = \{\mathbf{x}^{\text{obs}, i}\}_{i=1}^n$ or $\mathcal{D} = \{\mathbf{x}^{\text{obs}, i}, \mathbf{m}^i\}_{i=1}^n$. We also have a model to be optimized, denoted by $p_{\theta, \phi}(\mathbf{x}, \mathbf{m})$. Our goals can then be described as follows:

- To find a new framework to model the joint distribution of \mathbf{x} and \mathbf{m} , which better masters the MNAR mechanism. That is, we wish to learn ideal parameters θ and ϕ for the parametric model $p_{\theta, \phi}(\mathbf{x}, \mathbf{m})$ of a deep generative imputation model depending on a new decomposition of the joint distribution that avoids the previous pitfalls, such that $p_{\hat{\theta}, \hat{\phi}}(\mathbf{x}, \mathbf{m}) = p_{\mathcal{D}}(\mathbf{x}, \mathbf{m})$.

- Then, given the appropriate parameters, we are able to perform missing-data imputation by $\mathbb{E}[\mathbf{x}^{\text{mis}} | \mathbf{x}^{\text{obs}}, \mathbf{m}]$. If our parameter estimate is unbiased, then our imputation is also unbiased, i.e., $p_{\hat{\theta}, \hat{\phi}}(\mathbf{x}^{\text{mis}} | \mathbf{x}^{\text{obs}}, \mathbf{m}) = p_{\mathcal{D}}(\mathbf{x}^{\text{mis}} | \mathbf{x}^{\text{obs}}, \mathbf{m})$.

3 NON-NEGLIGIBLE MISSING MECHANISM MODELING

In general, we are interested in obtaining estimates of the parameters θ in the data model $p_{\theta}(\mathbf{x})$, via maximum likelihood estimation or Bayesian inference. But the assumptions about the missing mechanism determine the appropriate way to learn the data model. To maximize the likelihood of the parameter based only on observed quantities, the missing data is integrated out from the joint distribution, as:

$$\arg \max_{\theta} p_{\theta}(\mathbf{x}^{\text{obs}}, \mathbf{m}) = \arg \max_{\theta} \int p_{\theta}(\mathbf{x}^{\text{obs}}, \mathbf{x}^{\text{mis}}, \mathbf{m}) d\mathbf{x}^{\text{mis}}, \quad (5)$$

Reviewing the three types of missing mechanisms, if missing data is MCAR or MAR, we can maximize the maximum likelihood only based on observed data [27], i.e., $p_{\theta}(\mathbf{x}^{\text{obs}}, \mathbf{m}) \propto p_{\theta}(\mathbf{x}^{\text{obs}})$. But the above argument does not hold for MNAR data. The missing mechanism cannot be neglected during learning and has to be modeled within a joint distribution framework.

3.1 Existing MNAR modeling approaches

Little and Rubin [19] describe three ways of modeling the joint distribution of \mathbf{x} and \mathbf{m} in MNAR case.

Pattern mixture model [18], decomposes the joint distribution as Equation 6, where $p_\theta(\mathbf{m})$ is a Bernoulli distribution and $p_\phi(\mathbf{x}|\mathbf{m})$ is a mixture of distributions. The key issue is that it requires specifying the distribution of each missing pattern separately. And the data model is stratified by the different missing scenarios, leading to 2^d ($\mathbf{m} \in \mathbb{R}^d$) different conditional data models, which is unacceptable on a high-dimensional categorical variable. So it is not suitable for imputation tasks. Moreover mapping the mask which contains only binary information to the data space, obviously has an information bottleneck, and certainly affects the imputation effect of the model seriously. Collier et al. [5] are interested in learning a good generative model of \mathbf{x}^{obs} and as a result, propose a special *pattern mixture model* based method.

$$p_{\theta,\phi}(\mathbf{x}, \mathbf{m}) = p_\theta(\mathbf{m}) p_\phi(\mathbf{x}|\mathbf{m}). \quad (6)$$

Selection model [9], is the mainstream probability decomposition of the joint distribution (Equation 7). It models the distribution of the data and the incidence of missing data (the mask, \mathbf{m}) as a function of \mathbf{x} . One of our main baseline methods, not-MIWAE [12], is a selection-model-based method that uses VAEs to model $p_\theta(\mathbf{x})$ and an additional block (e.g., a single layer neural network) to model $p_\phi(\mathbf{m}|\mathbf{x})$ behind VAEs. The empirical results of Ghalebikesabi et al. [6] show that Not-MIWAE is less robust to possible missing cases. Moreover, allowing the missing model $p_\phi(\mathbf{m}|\mathbf{x})$ to be parameterized by a neural network has the disadvantage that the fit of $p_\theta(\mathbf{x})$ suffers from the flexibility of the missing model. In the case that the sparsity of data is high, $p_\phi(\mathbf{m}|\mathbf{x})$ dominates the model, and the reconstruction of observed data is despised.

$$p_{\theta,\phi}(\mathbf{x}, \mathbf{m}) = p_\theta(\mathbf{x}) p_\phi(\mathbf{m}|\mathbf{x}). \quad (7)$$

Furthermore, we find the reconstructed mask is always biased and argue that this pitfall is inevitable. We assume that the model is capable to capture both distributions of observed and missing data. The mask reconstruction is essentially solving a classification problem. However, the difference is that traditional classification tasks are sample-level and can make use of rich information from multiple feature spaces, while mask reconstruction depends on each data point with very little information available. Moreover, the sample points have obvious clustering characteristics by category in high-dimensional feature spaces, while the observed and missing values in the data point space are highly overlapping in distribution with the same domains of values (Rating 1-5) and similar probability to be observed or missing (Rating 2-4) in Figure 1. Thus the imputed data cannot be precisely divided into observed data and missing data by a simple mapping.

Pattern-set mixture model combines the two methods mentioned above (Equation 8) [18]. \mathbf{r} is an additional categorical latent variable that clusters the missing patterns into k missing pattern sets. k depends on the missing types where the missing data suffers. Therefore it is difficult to set up an appropriate value for k . In a special case where $k = 1$, it reduces to the selection model. PSM-VAE [6] can be categorized as a pattern-set mixture model. The pattern-set mixture model is a clustering variant of the selection model. The pitfalls we analyzed in the *selection model* are also in

the pattern-set mixture model.

$$p_{\lambda,\theta,\phi}(\mathbf{x}, \mathbf{m}, \mathbf{r}) = p_\lambda(\mathbf{r}) p_\theta(\mathbf{x}|\mathbf{r}) p_\phi(\mathbf{m}|\mathbf{x}, \mathbf{r}). \quad (8)$$

3.1.1 Serial-structure models.

The above three statistical methods have similarities in serial-structure modeling. All of them first model a distribution of one modality ($p_\theta(\mathbf{x})$, $p_\theta(\mathbf{m})$ or $p_\theta(\mathbf{x}|\mathbf{r})$), and then utilize the serial structure to model the conditional distribution of the other modality depending on the former ($p_\phi(\mathbf{m}|\mathbf{x})$, $p_\phi(\mathbf{x}|\mathbf{m})$ or $p_\phi(\mathbf{m}|\mathbf{x}, \mathbf{r})$). We call the above three methods the *serial models*. Briefly, these serial models cannot extract rich information in both data space and mask space which leads to biased imputation performance.

3.2 Parallel-structure conjunction model

Now that \mathbf{x} and \mathbf{m} have their unique information and cannot be transformed between each other. From the perspective of multimodal deep learning, we regard the joint distribution modeling of \mathbf{x} and \mathbf{m} as learning a joint representation of two modalities of missing-data multimodality. Under this assumption, we propose a new generative-model-specific probabilistic decomposition method to model the joint distribution in parameters, as:

$$p_{\theta,\phi}(\mathbf{x}, \mathbf{m}, \mathbf{u}) = p_\theta(\mathbf{u}) p_\phi(\mathbf{m}, \mathbf{x}|\mathbf{u}). \quad (9)$$

The detail is that we assume an auxiliary variable \mathbf{u} for the intermediate fusion layer, which has integrated information of multiple modalities, like a joint representation embedding. The fusion layer allows us to capture complementary information about the missing mechanism, which is not visible in individual modalities themselves. The prior information can be injected through \mathbf{u} .

$$p_{\theta,\phi}(\mathbf{x}, \mathbf{m}, \mathbf{u}) = p_\theta(\mathbf{u}) p_{\phi_1}(\mathbf{x}|\mathbf{u}) p_{\phi_2}(\mathbf{m}|\mathbf{u}). \quad (10)$$

MNAR mechanism has so many cases depending on the different relationships between elements of \mathbf{x} and \mathbf{m} . To account for complicated MNAR scenarios and to improve the robustness of model specification, we assume that \mathbf{x} and \mathbf{m} are independent conditional on the joint representation \mathbf{u} , which is more reasonable for the two modalities. More specifically, θ is a shared parameter, but ϕ is not. $p_{\phi_1}(\mathbf{x}|\mathbf{u})$ and $p_{\phi_2}(\mathbf{m}|\mathbf{u})$ are two parameter models with different parameters (i.e., two parallel neural networks in practical). On the other hand, the **parallel architecture** avoids the nuisance suffered by serial models. The new joint model can be presented as Equation 10, namely the **conjunction model**. Depending on the flexibility of parallel structure, the conjunction model can extract the rich information in both data space and mask space and generalize kinds of MNAR scenarios, not just self-masking scenarios.

4 GNR: A DEEP GENERATIVE IMPUTATION MODEL FOR MNAR DATA

In the previous section, we analyze the existing approaches to model the missing mechanism and propose the conjunction model. However, we still need to derive a practical algorithm that is flexible and compatible with our assumptions. In this section, we propose **GNR**, a deep generative imputation model for MNAR data based on the conjunction model (Figure 3), which can handle general MNAR scenarios with a large range of missing proportions.

4.1 Deep generative conjunction model

We now define a generative model for $p_{\theta, \phi}(\mathbf{x}, \mathbf{m})$. The parameters of the joint distribution need to be optimized jointly in an MNAR setting. To maximize the likelihood of the parameters (θ, ϕ) based only on observed quantities, the missing data is integrated out from the joint distribution given by:

$$p_{\theta, \phi}(\mathbf{x}^{\text{obs}}, \mathbf{m}) = \int p_{\phi}(\mathbf{x}^{\text{obs}}, \mathbf{x}^{\text{mis}}, \mathbf{m}) d\mathbf{x}^{\text{mis}}. \quad (11)$$

Introducing the conjunction model in the form of Equation 10, we can rewrite Equation 11 as:

$$p_{\theta, \phi}(\mathbf{x}^{\text{obs}}, \mathbf{m}) = \int p_{\phi_1}(\mathbf{x}|\mathbf{u}) p_{\phi_2}(\mathbf{m}|\mathbf{u}) p_{\theta}(\mathbf{u}) d\mathbf{x}^{\text{mis}} d\mathbf{u}, \quad (12)$$

where the parameters of the missing-data model and the parameters of the missing-mask model are tied together by \mathbf{u} . Then we introduce a latent variable \mathbf{z} :

$$p_{\theta, \phi}(\mathbf{x}^{\text{obs}}, \mathbf{m}) = \int p_{\phi_1}(\mathbf{x}|\mathbf{u}, \mathbf{z}) p_{\phi_2}(\mathbf{m}|\mathbf{u}, \mathbf{z}) p_{\theta}(\mathbf{u}|\mathbf{z}) p(\mathbf{z}) d\mathbf{x}^{\text{mis}} d\mathbf{u} d\mathbf{z}. \quad (13)$$

The integral in Equation 13 is analytically intractable, and direct maximum likelihood methods for learning the parameters (θ, ϕ) are inapplicable. We utilize *importance weighted variational inference* [2] to approximate the integral, turning the estimate of a likelihood to the lower bound of the likelihood in an unbiased way. Technically, we introduce an amortized variational inference network $q_{\gamma}(\mathbf{z}|\mathbf{x}^{\text{obs}})$, which comes from a simple family (e.g., the Gaussian family), and its parameter γ is learnable through a neural network. The issue is that a neural network cannot deal with variable length input. Nazabal et al. [26] use zero imputation (ZI) which first fills the missing value with zero and then feeds the imputed data as input for the inference network. Ma et al. [21] use a permutation invariant set function with the ability to handle the input in variable length. The empirical results show that the effects are similar and we choose the latter. Introducing the variational distribution $q_{\gamma}(\mathbf{z}|\mathbf{x}^{\text{obs}})$, and using the assumption that: $p_{\theta}(\mathbf{x}|\mathbf{u}, \mathbf{z}) = p_{\theta}(\mathbf{x}^{\text{obs}}|\mathbf{u}, \mathbf{z}) p_{\theta}(\mathbf{x}^{\text{mis}}|\mathbf{u}, \mathbf{z})$, Equation 13 is equal to:

$$\begin{aligned} & \log p_{\theta, \phi}(\mathbf{x}^{\text{obs}}, \mathbf{m}) \\ &= \log \int \frac{p_{\phi_1}(\mathbf{x}^{\text{obs}}|\mathbf{u}, \mathbf{z}) p_{\phi_2}(\mathbf{m}|\mathbf{u}, \mathbf{z}) p_{\theta}(\mathbf{u}|\mathbf{z}) p(\mathbf{z})}{q_{\gamma}(\mathbf{z}|\mathbf{x}^{\text{obs}})} \\ & \quad q_{\gamma}(\mathbf{z}|\mathbf{x}^{\text{obs}}) p_{\phi_1}(\mathbf{x}^{\text{mis}}|\mathbf{u}, \mathbf{z}) d\mathbf{x}^{\text{mis}} d\mathbf{u} d\mathbf{z} \\ &= \log \mathbb{E}_{\mathbf{z} \sim q_{\gamma}(\mathbf{z}|\mathbf{x}^{\text{obs}}), \mathbf{x}^{\text{mis}} \sim p_{\phi_1}(\mathbf{x}^{\text{mis}}|\mathbf{u}, \mathbf{z})} \left[\frac{p_{\phi_1}(\mathbf{x}^{\text{obs}}|\mathbf{u}, \mathbf{z}) p_{\phi_2}(\mathbf{m}|\mathbf{u}, \mathbf{z}) p_{\theta}(\mathbf{u}|\mathbf{z}) p(\mathbf{z})}{q_{\gamma}(\mathbf{z}|\mathbf{x}^{\text{obs}})} \right]. \end{aligned} \quad (14)$$

The prior information can be added to the model by obtaining prior embedding from a prior network and injecting it into the latent space through \mathbf{u} . If no extra information can be introduced, we can select the low-sparsity samples or features as the heuristic prior or even omit \mathbf{u} under the assumption that \mathbf{z} has learned all the latent representation we need. Since \mathbf{u} is an auxiliary variable,

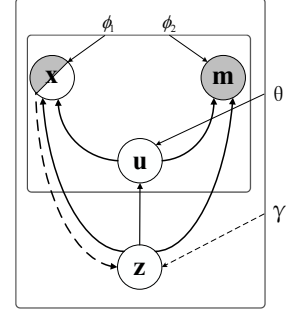


Figure 3: Graphical representation of GNR.

we do not need to use a large number of samples to estimate its expectation. We replace other expectations inside the logarithm with Monte Carlo estimates. Let

$$\mathcal{L}_K(\theta, \phi, \gamma) = \mathbb{E}_{\{z^k, \mathbf{x}^{\text{mis}, k}\}_{k \in \{1, \dots, K\}}} \left[\log \frac{1}{K} \sum_{k=1}^K \omega_k \right], \quad (15)$$

where, for all $k \leq K$, ω_k is the importance weight and calculated as:

$$\omega_k = \frac{p_{\phi_1}(\mathbf{x}^{\text{obs}}|\mathbf{u}, z^k) p_{\phi_2}(\mathbf{m}|\mathbf{u}, z^k) p_{\theta}(\mathbf{u}|z^k) p(z^k)}{q_{\gamma}(z^k|\mathbf{x}^{\text{obs}})}. \quad (16)$$

$\{z^k, \mathbf{x}^{\text{mis}, k}\}$ are K i.i.d. samples from $q_{\gamma}(\mathbf{z}|\mathbf{x}^{\text{obs}})$ and $p_{\phi_1}(\mathbf{x}^{\text{mis}}|\mathbf{u}, z^k)$ through *reparameterization trick* [14]. Similar to the approach proposed in Ipsen et al. [12], we directly give the monotonicity property of \mathcal{L}_K and the convergence to the true likelihood in Equation 17. The unbiasedness of the Monte Carlo estimates ensures (via Jensen's inequality) that the objective is indeed a lower bound of the likelihood.

$$\mathcal{L}_1(\theta, \phi, \gamma) \leq \dots \leq \mathcal{L}_K(\theta, \phi, \gamma) \xrightarrow{K \rightarrow \infty} \log p_{\theta, \phi}(\mathbf{x}^{\text{obs}}, \mathbf{m}), \quad (17)$$

where $\mathcal{L}_K(\theta, \phi, \gamma)$ is an unbiased importance weighted lower bound of $\log p_{\theta, \phi}(\mathbf{x}^{\text{obs}}, \mathbf{m})$, named **GNR lower bound**.

In addition, to handle a wide range of missing scenarios, we introduce a hyper-parameter α for $p_{\phi_2}(\mathbf{m}|\mathbf{u}, z^k)$ in Equation 18. α handles the trade-off between learning the model $p_{\phi_2}(\mathbf{m}|\mathbf{u}, z^k)$ that explains the missing mask better and learning the model $p_{\phi_1}(\mathbf{x}^{\text{obs}}|\mathbf{u}, z^k)$ that explains the observable variables better. When $\alpha = 1$, $\hat{\omega}$ is equivalent to ω . In a special condition, when $\alpha \rightarrow 0$, the model degenerates to a VAE similar to MIWAE [24], which can handle MCAR/MAR data.

$$\hat{\omega}_k = \frac{p_{\phi_1}(\mathbf{x}^{\text{obs}}|\mathbf{u}, z^k) \left[p_{\phi_2}(\mathbf{m}|\mathbf{u}, z^k) \right]^{\alpha} p_{\theta}(\mathbf{u}|z^k) p(z^k)}{q_{\gamma}(z^k|\mathbf{x}^{\text{obs}})}. \quad (18)$$

Note that we neither use two encoders to specifically encode \mathbf{x} and \mathbf{m} , nor concatenate them to feed one encoder. We do not include the missing mask \mathbf{m} as additional input to q_{γ} , as we want GNR to learn a convincing missing mask by itself through the MNAR mechanism. We can optimize the parameters θ, ϕ, γ by solving the

following optimization problem:

$$\theta^*, \phi^*, \gamma^* = \arg \max_{\theta, \phi, \gamma} \mathbb{E}_{(\mathbf{x}^{\text{obs}}, \mathbf{m}) \sim p_D(\mathbf{x}^{\text{obs}}, \mathbf{m})} \mathcal{L}_K(\theta, \phi, \gamma, \mathbf{x}^{\text{obs}}, \mathbf{m}). \quad (19)$$

Imputation. Given $\theta^*, \phi^*, \gamma^*$, we can impute the missing data by estimating $\mathbb{E}_{\mathbf{x}^{\text{mis}}} [h(\mathbf{x}^{\text{mis}}) | \mathbf{x}^{\text{obs}}, \mathbf{m}]$ using self-normalized importance sampling [12]. In the case that the l_2 norm is a relevant error metric, h is the identity function:

$$\begin{aligned} \hat{\mathbf{x}}^{\text{mis}} &= \mathbb{E}_{\mathbf{x}^{\text{mis}}} [h(\mathbf{x}^{\text{mis}}) | \mathbf{x}^{\text{obs}}, \mathbf{m}] \\ &\approx \sum_{l=1}^L \frac{\hat{\omega}_l}{\sum_{l=1}^L \hat{\omega}_l} \mathbb{E}_{\mathbf{x}^{\text{mis}}} [\mathbf{x}^{\text{mis}} | \mathbf{x}^{\text{obs}}, \mathbf{m}], \end{aligned} \quad (20)$$

where $L \gg K$. It is also possible to perform multiple imputations with the same computations. For this, we generate a set of imputations by using sampling importance resampling and weight them using the weights defined in Equation 20.

5 EXPERIMENTS

In this section, we quantitatively evaluate the imputation performance of our model and several state-of-the-art approaches on synthetic datasets (Section 5.1), real-world datasets with synthetic missing settings (Section 5.2), and real-world MNAR datasets with MCAR test sets (Section 5.3). The best score for each group is highlighted in **bold** and the next best is underlined.

The experimental setting details. We first introduce the general settings of GNR and other baselines. GNR is based on the *conjunction model* in Section 4. The data model ($p_{\phi_1}(\mathbf{x} | \mathbf{u}, \mathbf{z})$) for GNR is parameterized with Gaussian likelihood functions. The missing mask model ($p_{\phi_2}(\mathbf{x} | \mathbf{u}, \mathbf{z})$) uses Bernoulli likelihood and sigmoid activation. All the VAE-based approaches have two hidden layers with 128 nodes for both the encoder and decoder. All neural networks use Tanh activation except for output layers. Gaussian distributions are used as the variational distribution in the latent space. We use the Adam optimizer with a learning rate of 0.001 and train for 10k iterations with a batch size of 128. All VAE-based baselines use importance-weighted VAE objectives with $k = 20$ importance samples, and $L = 1000$ is used for estimating the imputation performance. All the code of MF-based methods can be found in Wang et al. [39].

Missing settings. We introduce synthetic missing data as follows: the MNAR data are generated by self-masking in **half of the features**: x_i is missing, if x_i is greater than the feature mean, with some certain probability (e.g., 20%, 80%, and 100%). In this case, the sparsity of a dataset with a k probability of missing is about $k/4$. The MCAR characteristic is introduced by random masking in **all of the features** to be missing with some certain probability.

5.1 Synthetic MNAR dataset

First, to evaluate the superiority of our *conjunction model*, we consider a 4 d synthetic MNAR dataset ($\mathbf{x} \in \mathbb{R}^4$), which consists of samples from a multivariate Gaussian distribution and multiple missing cases. If the missing mechanism is MNAR, $\mathbf{x}_1, \mathbf{x}_2$ are self-masking, and $\mathbf{x}_3, \mathbf{x}_4$ are fully observed. We not only model MNAR but also created a version of the data set (the last column of Table 1) where all features are MCAR and half of the features are

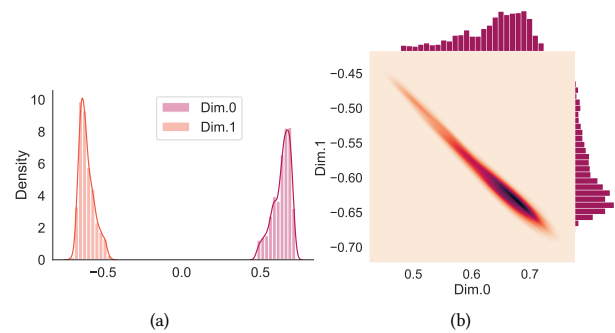


Figure 4: Visualization of latent space. (a): the value distribution of latent space after dimension reduction; (b): the smooth kernel density of the two dimensions in (a).

additionally MNAR. We use 1-dimensional latent space and zero imputation for the simple structure of synthetic data. The mean and standard errors are found over 5 runs. We compare GNR with the following baselines: i) MIWAE [24]: a VAE-based model specifically designed for MAR data with Zero Imputation; ii) not-MIWAE [12]: incorporating selection model into MIWAE for MNAR data; iii) PSM-VAE [6]: incorporating pattern-set mixture model into MIWAE; iv) traditional methods: mean imputation, MICE with Bayesian Ridge regression [36], and MissForest [34].

In Table 1, we first notice that MIWAE performs poorly on MNAR data, which indicates that a proper model of the missing mechanism is necessary for tackling the MNAR problem. Faced with multiple missing scenarios and mixed missing scenarios, our proposed GNR surpasses baselines with significant margins consistently (averagely improved by 13.3%), which verifies the validity of the proposed conjunction model for deep generative imputation models.

5.1.1 Visualization of latent space. The vanilla implementation of the VAE assumes a standard Gaussian marginal (prior) over latent variable \mathbf{z} . The latent variables (or aggregated posterior variables) are approximately isotropic standard Gaussian in each dimension. However, after the dimension reduction of latent variables in GNR, we generate two separate populations of posterior distributions with significantly different ranges in Figure 4(a). We argue that GNR couples the missing mechanism into latent representation, the two peaks in Figure 4(a) focus on missing values and observed values respectively. Each sample contains both observed and missing values, thus each sample has dual attributes responding to the two separate populations of posterior distributions. The kernel density in Figure 4(b) is not an ordinary radial circle representing each dimension independently and has structured information. We hypothesize that to prevent all the values in a sample fall into the missing-data modeling or observed-data modeling, the latent variables in different dimensions tend to separate.

5.2 Single imputation on UCI datasets

We compare different imputation methods on real-world datasets from the UCI repository [1]*. Similar to Ipsen et al. [12], we set the dimension of the latent space to $d - 1$ ($\mathbf{x} \in \mathbb{R}^d$), and use zero

*<https://archive-beta.ics.uci.edu/>

Table 1: Imputation RMSE for synthetic data under multiple missing scenarios. XX% is related to a probability of a value above the mean missing (MNAR). %Improv.:percentage of improvement on metrics over the best baseline.

Method	20%	80%	100%	★	80%+20%MCAR
MIWAE	1.06 +- 0.03	1.45 +- 0.01	1.71 +- 0.02	1.70 +- 0.02	1.27 +- 0.01
not-MIWAE	<u>0.94 +- 0.04</u>	1.26 +- 0.03	<u>1.33 +- 0.03</u>	1.38 +- 0.06	<u>1.16 +- 0.03</u>
PSMVAE	0.98 +- 0.02	<u>1.17 +- 0.03</u>	1.39 +- 0.03	<u>1.31 +- 0.07</u>	1.25 +- 0.02
GNR	0.87 +- 0.05	0.91 +- 0.03	1.14 +- 0.04	1.15 +- 0.06	1.04 +- 0.01
mean	1.05 +- 0.04	1.45 +- 0.01	1.71 +- 0.01	1.71 +- 0.01	1.26 +- 0.01
MICE	1.05 +- 0.04	1.45 +- 0.01	1.71 +- 0.01	1.71 +- 0.01	1.29 +- 0.04
MissForest	1.11 +- 0.05	1.49 +- 0.01	1.74 +- 0.02	1.76 +- 0.01	1.36 +- 0.03
%Improv.	+7.4%	+22.2%	+14.3%	+12.2%	+10.3%

★ : if first feature value $x_1 > \bar{x}_1$ (feature mean) or second feature value $x_2 < \bar{x}_2$, x_1/x_2 will be missing with 100% probability.

Table 2: Imputation RMSE on UCI datasets under different missing scenarios.

Method \ Dataset	white wine			abalone			banknote			Yeast			red wine			concrete		
	20%	80%	100%	20%	80%	100%	20%	80%	100%	20%	80%	100%	20%	80%	100%	20%	80%	100%
MIWAE	1.04	1.25	1.55	0.63	0.44	0.80	0.36	0.81	1.26	1.07	1.51	1.73	0.98	1.24	1.62	0.43	1.25	1.70
not-MIWAE	<u>0.91</u>	<u>1.04</u>	<u>1.18</u>	0.52	<u>0.43</u>	0.94	<u>0.31</u>	0.46	1.06	<u>0.97</u>	1.28	1.52	<u>0.90</u>	<u>1.07</u>	1.25	<u>0.42</u>	0.81	1.32
PSMVAE	0.94	1.09	1.21	<u>0.45</u>	0.47	<u>0.74</u>	0.33	<u>0.43</u>	<u>0.97</u>	0.99	<u>1.14</u>	<u>1.28</u>	0.92	1.19	<u>1.21</u>	0.56	<u>0.79</u>	<u>1.15</u>
GNR	0.87	0.93	1.02	0.33	0.41	0.47	0.30	0.40	0.72	0.84	0.87	0.98	0.84	1.04	1.14	0.40	0.69	1.06
%Improv.	+4.4%	+10.6%	+13.6%	+26.7%	+4.7%	+36.5%	+3.2%	+7.0%	+25.8%	+13.4%	+23.7%	+23.4%	+6.7%	+2.8%	+5.8%	+4.8%	+12.7%	+7.8%
mean	1.32	1.59	1.74	1.05	1.39	1.69	1.12	1.46	1.73	1.13	1.52	1.73	1.41	1.68	1.84	1.15	1.60	1.85
MICE	1.05	1.21	1.41	0.54	0.58	0.61	0.69	0.98	1.41	1.04	1.42	1.76	0.94	1.16	1.68	0.51	0.74	1.69
MissForest	0.82	1.15	1.63	0.53	0.55	1.32	0.35	0.74	1.28	1.05	1.43	1.71	0.81	1.09	1.64	0.32	0.78	1.76

Table 3: Reconstructed mask accuracy on UCI datasets under different missing scenarios. We only measure features that contain missing values. RANDOM means the accuracy lower bound of the mask which is generated completely randomly.

Method \ Dataset	white wine			abalone			banknote			yeast			red wine			concrete		
	20%	80%	100%	20%	80%	100%	20%	80%	100%	20%	80%	100%	20%	80%	100%	20%	80%	100%
RANDOM	82.00%	52.00%	50.00%	82.00%	52.00%	50.00%	82.00%	52.00%	50.00%	82.00%	52.00%	50.00%	82.00%	52.00%	50.00%	82.00%	52.00%	50.00%
not-MIWAE	84.23%	68.49%	78.52%	82.26%	74.43%	83.53%	83.12%	75.85%	72.48%	83.36%	56.34%	53.27%	86.19%	73.24%	83.53%	84.61%	70.75%	76.16%
GNR	93.54%	93.37%	96.42%	87.79%	88.82%	98.14%	84.79%	91.02%	93.44%	94.62%	89.76%	92.90%	88.77%	95.16%	95.12%	95.33%	96.48%	96.87%

imputation and standardization for each feature before the missing is introduced. Experiments are repeated 5 times.

The interrelationships between features are more complex in real-world datasets compared to synthetic datasets. GNR in Table 2 shows significant margins over other baselines clearly in multiple datasets (9.9%, 10.3%, and 18.8% respectively for 20%, 80%, and 100% missing probability). Similar to results in Ghalebikesabi et al. [6], traditional methods such as MissForest and MICE sometimes outperform neural network-based methods when the missing probability is low. But when we sample a single value from the predictive distribution of traditional methods, deep generative models outperform them. Another drawback of MICE and MissForest is that they are typically not scalable to high-dimensional datasets, while GNR can. The stable and superior performance compared to the baselines in different datasets with multiple missing probabilities demonstrates the broad applicability and robustness of our approach.

5.2.1 Studies of missing mask reconstruction. We also demonstrate the mask-reconstruction accuracy in Table 3. Firstly we assume the MCAR scenario that observed data and missing data have

the same distribution and randomly generate the reconstructed mask. To get the best accuracy, $\sum p(\mathbf{m} = 0) = k/4$, and $\sum p(\mathbf{m} = 1) = 1 - k/4$, must be satisfied (where k is the missing probability). In this case, the theoretical accuracy is $[k^2 + (1 - k/2)^2] * 100\%$, which is the lower bound of reconstructed mask accuracy. One of our core baselines, PSMVAE, is not compared because it uses both \mathbf{x} and \mathbf{m} as input. It is hard to figure out whether PSMVAE has learned the missing mechanism to build the missing mask or PSMVAE just recovers the inputted \mathbf{m} .

In Table 3, not-MIWAE usually gives a poor mask-reconstruction performance and is sometimes close to the lower bound (RANDOM), which means not-MIWAE fails to extract the information in the mask. The visualization in Figure 5(a) proves our point: not-MIWAE pushes some values, which are difficult to determine whether missing, to 0.5 (close to red) to reduce the global loss. GNR (Figure 5(b)) gives a convincing probabilistic mask that is similar to the ground truth (Figure 5(c)), which implies that GNR understands the missing mechanism from its learning process and makes the imputation task more principled. Taking Table 2 and Table 3 together, the parallel-structure GNR fully mines the information in incomplete data and

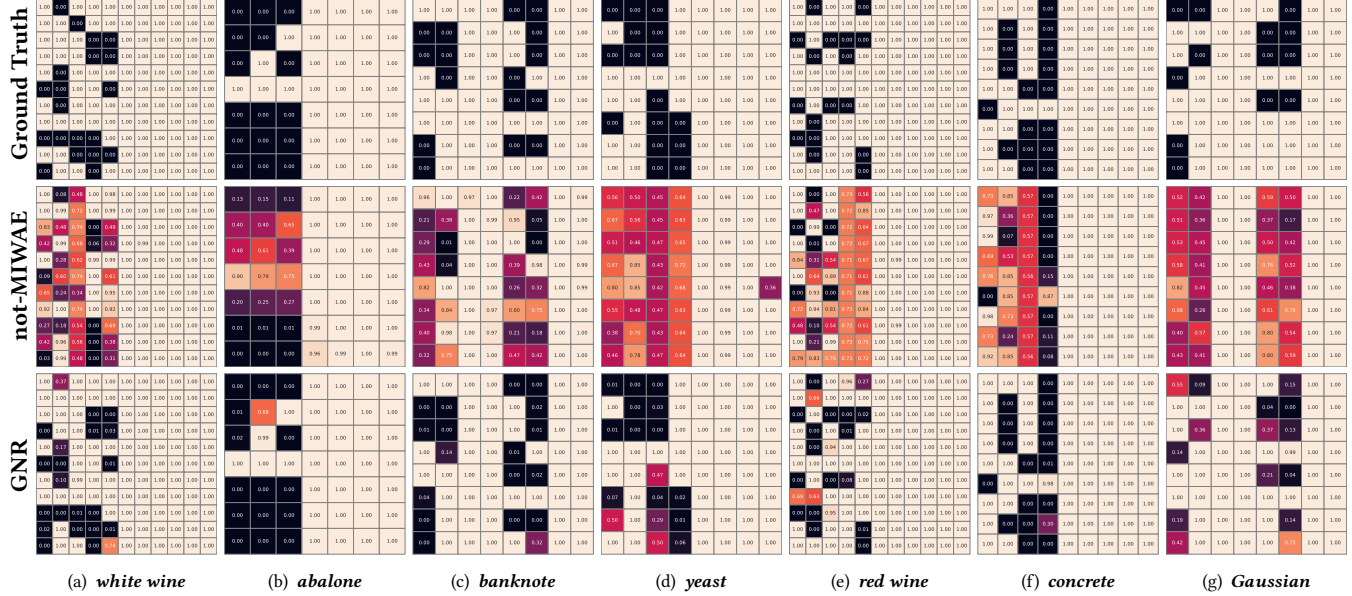


Figure 5: Random local details of the reconstructed undiscretized mask in 6 realistic datasets and 1 synthetic dataset. The value in the undiscretized mask can be considered as the probability that a value is observed, namely *probabilistic mask*.

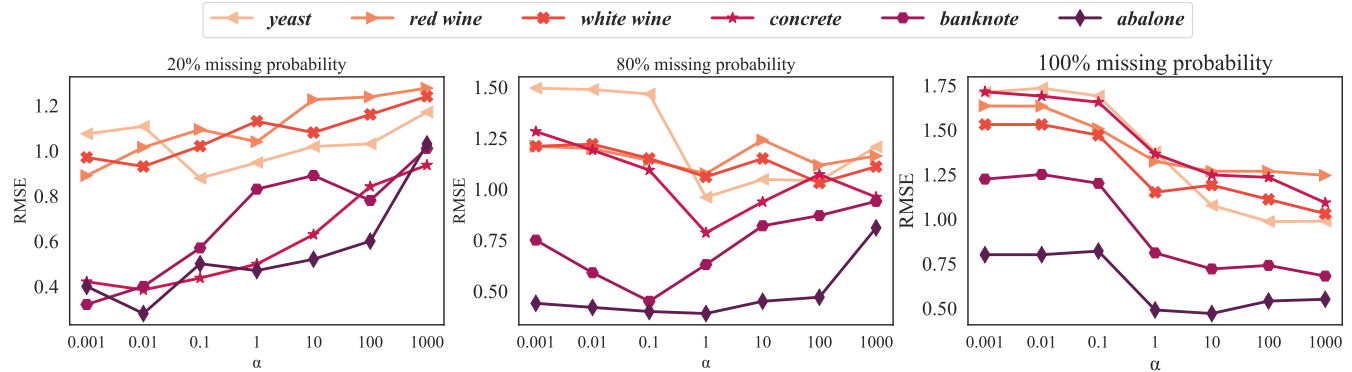


Figure 6: Performance comparisons with varying hyper-parameter values α on UCI datasets.

missing masks, and finally performs better than others. Note that even in some cases our GNR does not significantly outperform other baselines on global evaluation metrics, GNR still gives more reasonable estimates for each local missing value based on accurate mask reconstruction, and principled imputation results are more meaningful for downstream tasks.

5.2.2 Studies of hyper-parameter. As a proportionality coefficient, the optimal choice of α only depends on the specific missing scenario of the dataset instead of the network architecture of the practical algorithm. In Figure 6, datasets have different sensitivities to α because of complex interrelationships between their features. But we notice that for each dataset, the optimal choice of α is positively correlated with the missing probability. α balances a trade-off between the flexibility of the missing mask model and the distortion it induces in the data model when the data is MAR/MCAR. This can be explained by the fact that GNR needs to spend more effort to reconstruct a more realistic missing mask and limit the flexibility

of the missing mask model when the missing probability is high. On the contrary, in extreme cases where the MNAR mechanism induces little distortion to the data distribution, we do not even need a missing mask model ($\alpha \rightarrow 0$) and degenerate GNR to a model for MAR/MCAR data similar to MIWAE [24]. Note that for different application scenarios, we do not need a more detailed range of α , and directly select an approximate α from $\{0.01, 1, 100\}$ according to the sparsity of the dataset.

5.3 Imputation with MCAR test sets

We employ two datasets, *Yahoo!R3* and *Coat* (Figure 1), which contain an MNAR set and a small MCAR set:

- *Yahoo!R3* contains five-star user-song ratings. The MNAR training set contains more than 300K self-selected ratings from 15,400 users on 1,000 songs (with 0.94 sparsity). And the MCAR test set contains randomly selected ratings from 5,400 users on 10 random songs (with 0.99 sparsity).

• *Coat* contains five-star user-coat ratings from 290 Amazon Mechanical Turk workers on an inventory of 300 coats. The training set contains 6,500 MNAR ratings collected through self-selections by the Turk workers (with 0.92 sparsity). And the test set is MCAR collected by asking the Turk workers to rate 16 randomly selected coats (with 0.95 sparsity).

We train GNR and baselines on MNAR training sets and evaluate the imputation error on MAR test sets to get an unbiased estimate of the imputation error. We compare with more baselines:

- MF [15]: the basic matrix factorization model makes no further assumptions about the missing mechanism;
- MF-IPS and MF-SNIPS [29]: each data uses the inverse of its propensity score to weight for unbiased performance estimation;
- MF-DR and MF-DR-JL [37]: combining the propensity-scoring approach [29] with an error-imputation approach by Steck [33] to obtain a doubly robust estimator;
- MF-CVIB [39]: a counterfactual variational information bottleneck used for debiasing learning without MAR data;
- GAIN [40]: based on GANs, in which the generator outputs imputed data, and the discriminator determines which variables are observed based on partial information of the missing mask.

The propensity-based methods (MF-IPS, MF-SNIPS, MF-DR-JL) need access to a small sample of MAR data to estimate the propensities, which use 5% of the MAR test set for training. Similar to Ipsen et al. [12], we use the permutation invariant encoder [21] with an embedding size of 20 and a code size of 50, along with a linear mapping to a latent space of size 30. We use Equation 21 to preprocess the data, where $r \in \{1, 2, 3, 4, 5\}$ denotes a five-star rating. Additionally, ϵ controls the noise level in the grade information. We apply $\epsilon \sim N(0, 0.1)$ for training sets and $\epsilon = 0$ for test sets. The output layer has a sigmoid activation for the mean in the data model, scaled to match the scale of the inputs.

$$\hat{r} = \epsilon + (1 - \epsilon) \frac{2^r - 1}{2^{r_{\max}} - 1}. \quad (21)$$

Results are shown in Table 4. Our GNR outperforms all the baselines, and improvements are rather impressive — 12.0% and 8.3% in terms of *Yahoo!R3* and *Coat*. These results validate that GNR can better understand the MNAR mechanism and match the distribution of MCAR test sets. MNAR-based models generally outperform their MAR/MCAR versions (MIWAE, MF) for the appropriate assumption about the missing mechanism. And the propensity-based methods suffer from high variance and are difficult to develop a proper propensity score, which damages the performance. More importantly, among VAE-based models which use similar settings, GNR (based on the conjunction model) outperforms its selection model counterpart (not-MIWAE) and pattern-set mixture model counterpart (PSMVAE).

6 RELATED WORK

We briefly review methods that deal with MNAR data. Inverse propensity score (IPS) [10], a counterfactual technique, reweighting the collected data for expectation-unbiased learning, is taken to impute [3, 28, 39]. Sportisse et al. [32] and Ma and Chen [23], use low-rank models for estimation and imputation in MNAR settings. The causal approach is taken to the imputation task where MNAR

Table 4: Imputation MSE on *Yahoo!R3* and *Coat*.

Method	Family	<i>Yahoo!R3</i>	<i>Coat</i>
MIWAE		1.16	1.38
not-MIWAE	VAE	<u>1.08</u>	1.29
PSMVAE		1.13	<u>1.21</u>
GNR		0.95	1.11
MF		1.26	1.28
MF-IPS		1.18	1.33
MF-SNIPS	MF	1.10	1.23
MF-DR		1.15	1.31
MF-DR-JL		1.09	1.22
MF-CVIB		1.32	1.24
GAIN	GAN	1.11	1.23
%Improv.		+12.0%	+8.3%

is treated as a confounding bias [16, 38]. Muzellec et al. [25], use optimal transport to define a relevant loss for imputation.

Growing interest has been focused on applying deep generative models to missing-data imputation. Deep generative models such as generative adversarial nets (GANs) [8] or variational autoencoders (VAEs) [14] have been used for imputation since their introduction. Some methods use an extension of the variational lower bound to handle missing data under the MAR assumption [20, 21, 26]. Yoon et al. [40] and Li et al. [17] use GANs for imputing MCAR data. Diffusion models [11, 30] are also used for time series data imputation [35] under MAR assumption. More recently, deep generative models under MNAR have been studied. Gong et al. [7] and Ipsen et al. [12] are based on the selection model. Ma and Zhang [22] provide an identifiable deep generative selection model for MNAR data. Collier et al. [5] are based on the pattern mixture model. Ghalebikesabi et al. [6] build an idea from the pattern-set mixture model and introduce a probabilistic semi-supervised approach.

7 CONCLUSION

In this work, we propose principled solutions from the perspectives of modeling the MNAR mechanism and application area. First, we exemplarily explain some statistical MNAR modeling approaches and point out the inherent flaws in existing deep generative imputation models. Second, we propose a new MNAR modeling approach, the conjunction model, which views the complete data and the missing mask as two modalities of missing-data multimodality from a novel multimodal perspective. Third, we propose a practical algorithm, GNR, which fully mines the information in the two modalities without interfering with each other. The visualization of the reconstructed mask and latent variable, and the study of the hyper-parameter provide interpretability to GNR. Finally, we demonstrate that our method gains a significant and robust improvement over existing baselines on imputation tasks under various missing settings for both synthetic and real-world datasets.

For future work, we are interested in several extensions: (i) extending GNR to deep supervised learning; (ii) introducing identifiability and causal discovery to GNR [13]; (iii) modeling the conjunction model based on the deep diffusion models [11, 31].

REFERENCES

- [1] Arthur Asuncion and David Newman. 2007. UCI machine learning repository.
- [2] Yuri Burda, Roger B. Grosse, and Ruslan Salakhutdinov. 2016. Importance Weighted Autoencoders. In *4th International Conference on Learning Representations, ICLR 2016, San Juan, Puerto Rico, May 2-4, 2016, Conference Track Proceedings*.
- [3] Jiawei Chen, Hande Dong, Yang Qiu, Xiangnan He, Xin Xin, Liang Chen, Guli Lin, and Keping Yang. 2021. AutoDebias: Learning to debias for recommendation. In *Proceedings of the 44th International ACM SIGIR Conference on Research and Development in Information Retrieval*.
- [4] Jiawei Chen, Hande Dong, Xiang Wang, Fuli Feng, Meng Wang, and Xiangnan He. 2023. Bias and debias in recommender system: A survey and future directions. *ACM Transactions on Information Systems* 41, 3 (2023), 1–39.
- [5] Mark Collier, Alfredo Nazabal, and Christopher KI Williams. 2020. VAEs in the presence of missing data. *arXiv preprint arXiv:2006.05301* (2020).
- [6] Sahra Ghalebikesabi, Rob Cornish, Chris Holmes, and Luke J. Kelly. 2021. Deep Generative Missingness Pattern-Set Mixture Models. In *The 24th International Conference on Artificial Intelligence and Statistics, AISTATS 2021, April 13-15, 2021, Virtual Event (Proceedings of Machine Learning Research, Vol. 130)*. PMLR.
- [7] Yu Gong, Hossein Hajimirsadeghi, Jiawei He, Thibaut Durand, and Greg Mori. 2021. Variational Selective Autoencoder: Learning from Partially-Observed Heterogeneous Data. In *The 24th International Conference on Artificial Intelligence and Statistics, AISTATS 2021, April 13-15, 2021, Virtual Event (Proceedings of Machine Learning Research, Vol. 130)*. PMLR.
- [8] Ian J. Goodfellow, Jean Pouget-Abadie, Mehdi Mirza, Bing Xu, David Warde-Farley, Sherjil Ozair, Aaron C. Courville, and Yoshua Bengio. 2014. Generative Adversarial Nets. In *Advances in Neural Information Processing Systems 27: Annual Conference on Neural Information Processing Systems 2014, December 8-13 2014, Montreal, Quebec, Canada*.
- [9] James J Heckman. 1979. Sample selection bias as a specification error. *Econometrica: Journal of the econometric society* (1979).
- [10] José Miguel Hernández-Lobato, Neil Houlsby, and Zoubin Ghahramani. 2014. Probabilistic Matrix Factorization with Non-random Missing Data. In *Proceedings of the 31th International Conference on Machine Learning, ICML 2014, Beijing, China, 21-26 June 2014 (JMLR Workshop and Conference Proceedings, Vol. 32)*. JMLR.org.
- [11] Jonathan Ho, Ajay Jain, and Pieter Abbeel. 2020. Denoising Diffusion Probabilistic Models. In *Advances in Neural Information Processing Systems 33: Annual Conference on Neural Information Processing Systems 2020, NeurIPS 2020, December 6-12, 2020, virtual*.
- [12] Niels Bruun Ipsen, Pierre-Alexandre Mattei, and Jes Frellesen. 2020. not-MIWAE: Deep generative modelling with missing not at random data. *arXiv preprint arXiv:2006.12871* (2020).
- [13] Ilyes Khemakhem, Diederik Kingma, Ricardo Monti, and Aapo Hyvarinen. 2020. Variational autoencoders and nonlinear ica: A unifying framework. In *International Conference on Artificial Intelligence and Statistics*. PMLR.
- [14] Diederik P. Kingma and Max Welling. 2014. Auto-Encoding Variational Bayes. In *2nd International Conference on Learning Representations, ICLR 2014, Banff, AB, Canada, April 14-16, 2014, Conference Track Proceedings*.
- [15] Yehuda Koren, Robert Bell, and Chris Volinsky. 2009. Matrix factorization techniques for recommender systems. *Computer* 42, 8 (2009).
- [16] Trent Kyono, Yao Zhang, Alexis Bellot, and Mihaela van der Schaar. 2021. MIRA-CLE: Causally-Aware Imputation via Learning Missing Data Mechanisms. *Advances in Neural Information Processing Systems* 34 (2021).
- [17] Steven Cheng-Xian Li, Bo Jiang, and Benjamin M. Marlin. 2019. MisGAN: Learning from Incomplete Data with Generative Adversarial Networks. In *7th International Conference on Learning Representations, ICLR 2019, New Orleans, LA, USA, May 6-9, 2019*. OpenReview.net.
- [18] Roderick JA Little. 1993. Pattern-mixture models for multivariate incomplete data. *J. Amer. Statist. Assoc.* 88, 421 (1993).
- [19] Roderick JA Little and Donald B Rubin. 2019. *Statistical analysis with missing data*. Vol. 793. John Wiley & Sons.
- [20] Chao Ma, Wenbo Gong, José Miguel Hernández-Lobato, Noam Koenigstein, Sebastian Nowozin, and Cheng Zhang. 2018. Partial VAE for hybrid recommender system. In *NIPS Workshop on Bayesian Deep Learning*. Vol. 2018.
- [21] Chao Ma, Sebastian Tschiatschek, Konstantina Palla, José Miguel Hernández-Lobato, Sebastian Nowozin, and Cheng Zhang. 2019. EDDI: Efficient Dynamic Discovery of High-Value Information with Partial VAE. In *Proceedings of the 36th International Conference on Machine Learning, ICML 2019, 9-15 June 2019, Long Beach, California, USA (Proceedings of Machine Learning Research, Vol. 97)*. PMLR.
- [22] Chao Ma and Cheng Zhang. 2021. Identifiable Generative Models for Missing Not at Random Data Imputation. *Advances in Neural Information Processing Systems* 34 (2021).
- [23] Wei Ma and George H. Chen. 2019. Missing Not at Random in Matrix Completion: The Effectiveness of Estimating Missingness Probabilities Under a Low Nuclear Norm Assumption. In *Advances in Neural Information Processing Systems 32: Annual Conference on Neural Information Processing Systems 2019, NeurIPS 2019, December 8-14, 2019, Vancouver, BC, Canada*.
- [24] Pierre-Alexandre Mattei and Jes Frellesen. 2019. MIWAE: Deep Generative Modelling and Imputation of Incomplete Data Sets. In *Proceedings of the 36th International Conference on Machine Learning, ICML 2019, 9-15 June 2019, Long Beach, California, USA (Proceedings of Machine Learning Research, Vol. 97)*. PMLR.
- [25] Boris Muzellec, Julie Josse, Claire Boyer, and Marco Cuturi. 2020. Missing data imputation using optimal transport. In *International Conference on Machine Learning*. PMLR.
- [26] Alfredo Nazabal, Pablo M Olmos, Zoubin Ghahramani, and Isabel Valera. 2020. Handling incomplete heterogeneous data using vaes. *Pattern Recognition* 107 (2020).
- [27] Donald B Rubin. 1976. Inference and missing data. *Biometrika* 63, 3 (1976).
- [28] Yuta Saito. 2020. Asymmetric Tri-training for Debiasing Missing-Not-At-Random Explicit Feedback. In *Proceedings of the 43rd International ACM SIGIR conference on research and development in Information Retrieval, SIGIR 2020, Virtual Event, China, July 25-30, 2020*. ACM. <https://doi.org/10.1145/3397271.3401114>
- [29] Tobias Schnabel, Adith Swaminathan, Ashudeep Singh, Navin Chandak, and Thorsten Joachims. 2016. Recommendations as Treatments: Debiasing Learning and Evaluation. In *Proceedings of the 33rd International Conference on Machine Learning, ICML 2016, New York City, NY, USA, June 19-24, 2016 (JMLR Workshop and Conference Proceedings, Vol. 48)*. JMLR.org.
- [30] Yang Song and Stefano Ermon. 2019. Generative Modeling by Estimating Gradients of the Data Distribution. In *Advances in Neural Information Processing Systems 32: Annual Conference on Neural Information Processing Systems 2019, NeurIPS 2019, December 8-14, 2019, Vancouver, BC, Canada*.
- [31] Yang Song, Jascha Sohl-Dickstein, Diederik P Kingma, Abhishek Kumar, Stefano Ermon, and Ben Poole. 2020. Score-based generative modeling through stochastic differential equations. *arXiv preprint arXiv:2011.13456* (2020).
- [32] Aude Sportisse, Claire Boyer, and Julie Josse. 2020. Imputation and low-rank estimation with missing not at random data. *Statistics and Computing* 30, 6 (2020).
- [33] Harald Steck. 2013. Evaluation of recommendations: rating-prediction and ranking. In *Proceedings of the 7th ACM conference on Recommender systems*. 213–220.
- [34] Daniel J Stekhoven and Peter Bühlmann. 2012. MissForest—non-parametric missing value imputation for mixed-type data. *Bioinformatics* 28, 1 (2012).
- [35] Yusuke Tashiro, Jiaming Song, Yang Song, and Stefano Ermon. 2021. CSDI: Conditional score-based diffusion models for probabilistic time series imputation. *Advances in Neural Information Processing Systems* 34 (2021), 24804–24816.
- [36] Stef Van Buuren and Karin Groothuis-Oudshoorn. 2011. mice: Multivariate imputation by chained equations in R. *Journal of statistical software* 45 (2011).
- [37] Xiaojie Wang, Rui Zhang, Yu Sun, and Jianzhong Qi. 2019. Doubly Robust Joint Learning for Recommendation on Data Missing Not at Random. In *Proceedings of the 36th International Conference on Machine Learning, ICML 2019, 9-15 June 2019, Long Beach, California, USA (Proceedings of Machine Learning Research, Vol. 97)*. PMLR.
- [38] Yixin Wang and David M Blei. 2019. The blessings of multiple causes. *J. Amer. Statist. Assoc.* 114, 528 (2019).
- [39] Zifeng Wang, Xi Chen, Rui Wen, Shao-Lun Huang, Ercan Kuruoglu, and Yefeng Zheng. 2020. Information theoretic counterfactual learning from missing-not-at-random feedback. *Advances in Neural Information Processing Systems* 33 (2020).
- [40] Jinsung Yoon, James Jordon, and Mihaela van der Schaar. 2018. GAIN: Missing Data Imputation using Generative Adversarial Nets. In *Proceedings of the 35th International Conference on Machine Learning, ICML 2018, Stockholm, Sweden, July 10-15, 2018 (Proceedings of Machine Learning Research, Vol. 80)*. PMLR.